Contribution from the Department of Chemistry,
Purdue University, West Lafayette, Indiana 47907

Non-Metal Redox Kinetics: Hypobromite and Hypobromous Acid Reactions with Iodide and with Sulfite and the Hydrolysis of Bromosulfate

Robert C. Troy and Dale W. Margerum*

Received July 27, 1990

The pulsed-accelerated-flow method is used to study the reactions of OBr^- with I^- and with SO_3^{2-} (25.0 °C, μ = 0.50 M). Pseudo-first-order rate constants for the OBr^- with I^- reaction are measured in the range 5930–12900 s^{-1}. The even faster reaction between OBr^- and SO_3^{2-} is studied under second-order conditions. The proposed mechanism includes parallel paths with Br^+ transfer to the nucleophile ($X = I^-, SO_3^{2-}$) via solvent-assisted reaction with OBr^- as well as diffusion-controlled reactions between

$$H_2O + OBr^- + X \xrightarrow{k_{OBr}} XBr + 2OH^-$$

$$OBr^- + H_2O \underset{k_{-a}}{\overset{k_a}{\rightleftharpoons}} HOBr + OH^-$$

$$HOBr + X \xrightarrow{k_{HOBr}} XBr + OH^-$$

HOBr (pK_a = 8.80) and these nucleophiles. The second-order rate constants (M^{-1} s^{-1}) are as follows: k_{OBr} = 6.8 (±0.4) × 10^5 and k_{HOBr} = 5.0 (±0.3) × 10^9 with I^-; k_{OBr} = 1.0 (±0.1) × 10^8 and k_{HOBr} = 5 (±1) × 10^9 with SO_3^{2-}. The intermediate IBr(aq) is unstable with respect to hydrolysis, and it readily forms OI^-. The $BrSO_3^-$ that is formed in the OBr^- and HOBr reactions with SO_3^{2-} hydrolyzes with a rate constant k_h = 230 (±20) s^{-1} at 0.0 °C to give SO_4^{2-} and Br^-. The relative hydrolysis rate constants (25 °C) for the halosulfates are in the order $BrSO_3^- \gg ISO_3^- \simeq ClSO_3^- \gg FSO_3^-$.

Introduction

The kinetics and mechanisms of hypochlorous acid and hypochlorite ion reactions with iodide ion and with sulfite ion have been studied recently.[1-4] The OCl^- reactions were measured by stopped-flow spectrometry, but the HOCl reactions were more rapid and pulsed-accelerated-flow (PAF)[5-7] methods were needed. Chlorosulfate ion is formed from the reaction of HOCl and SO_3^{2-}, and the hydrolysis rate constant for $ClSO_3^-$ has been determined.[4] The formation of $ClSO_3^-$ shows that the reaction takes place by a Cl^+-transfer mechanism rather than an O atom transfer mechanism.

Hypobromite is not as strong an oxidizing agent as hypochlorite (eqs 1 and 2), but the present work shows that OBr^- reacts 3–5 orders of magnitude faster with SO_3^{2-} and with I^- than does OCl^-.

$$OBr^- + H_2O + 2e \rightarrow Br^- + 2OH^- \qquad E_b° = 0.766\ V \quad (1)$$

$$OCl^- + H_2O + 2e \rightarrow Cl^- + 2OH^- \qquad E_b° = 0.890\ V \quad (2)$$

Lister and McLeod[8] observed that the reactions of OBr^- with NO_2^- and with HCO_2^- have an inverse dependence in OH^- concentration, and they proposed HOBr as the reactant. Their equations imply that O atom transfer occurs in both cases. We also find that HOBr reacts very rapidly (near the diffusion limit) with I^- and with SO_3^{2-}, but we propose that the reactions occur by Br^+-transfer processes to form IBr and $BrSO_3^-$ as the first step in the redox mechanisms.

Iodine monobromide has been proposed as an intermediate in the reaction of HOBr, I^-, and H^+ from studies of oscillating reaction mechanisms.[9] The kinetics of IBr(aq) + I^- and the hydrolysis reactions of IBr(aq) in base have been studied recently[10] by use of the PAF method. (Solutions of IBr_2^- and Br^- were used to control the initial concentration of IBr(aq).) The hydrolysis rate constants (25.0 °C) for eq 3 (8 × 10^5 s^{-1}) and eq 4 (6.0 × 10^9 M^{-1} s^{-1}) are very large, so that IBr(aq) is only a transitory intermediate in the reactions of HOBr and OBr^- with I^-.

$$IBr(aq) + H_2O \rightarrow HOI + Br^- + H^+ \quad (3)$$

$$IBr(aq) + OH^- \rightarrow HOI + Br^- + H_2O \quad (4)$$

On the other hand, bromosulfate is formed in the reaction between sulfite and hypobromous acid (eq 5), and it hydrolyzes (eq 6) less rapidly so that the hydrolysis can be observed with use of an acid–base indicator by stopped-flow methods near 0 °C.

$$HOBr + SO_3^{2-} \rightarrow OH^- + BrSO_3^- \quad (5)$$

$$BrSO_3^- + H_2O \rightarrow Br^- + SO_4^{2-} + 2H^+ \quad (6)$$

Many non-metal redox reactions are too fast to measure by stopped-flow methods and are irreversible so that relaxation methods are not appropriate. The pulsed-accelerated-flow method overcomes these limitations and permits reactions to be studied that have half-lives as short as a few microseconds. The PAF method is used in this work to measure rate constants for the reactions of OBr^- and HOBr with I^- and with SO_3^{2-}.

Experimental Section

Reagents. Analytical reagent grade Br_2, NaI, and NaOH were used without further purification. Crystalline I_2 (resublimed) was dissolved in 1 mM $HClO_4$ and was standardized spectrophotometrically (λ = 460 nm, ϵ = 746 M^{-1} cm^{-1}).[11] $NaClO_4$ was recrystallized from water, and a 5 M stock solution was prepared, which was standardized gravimetrically. Hypobromite solutions (4.0 × 10^{-4} M) were prepared by addition of Br_2(l) to ice-cold NaOH solutions. A reference solution was standardized by an iodometric titration method, and the OBr^- molar absorptivity was determined as 332 (±1) M^{-1} cm^{-1} at 329 nm (λ_{max}). Subsequently, each NaOBr solution was freshly prepared, calibrated at 329 nm, and used within 2 h to prevent any significant disproportionation reactions.[12] A saturated NaOH solution was used to reduce CO_3^{2-} contamination and was diluted in deionized, distilled water that had been boiled and cooled under Ar. This NaOH stock solution was stored under

(1) Kumar, K.; Day, R. A.; Margerum, D. W. *Inorg. Chem.* **1986**, *25*, 4244-4350.
(2) Nagy, J. C.; Kumar, K.; Margerum, D. W. *Inorg. Chem.* **1988**, *27*, 2773-2780.
(3) Fogelman, K. D.; Walker, D. M.; Margerum, D. W. *Inorg. Chem.* **1989**, *28*, 986-993.
(4) Yiin, B. S.; Margerum, D. W. *Inorg. Chem.* **1988**, *27*, 1670-1672.
(5) Jacobs, S. A.; Nemeth, M. T.; Kramer, G. W.; Ridley, T. Y.; Margerum, D. W. *Anal. Chem.* **1984**, *56*, 1058-1065.
(6) Nemeth, M. T.; Fogelman, K. D.; Ridley, T. Y.; Margerum, D. W. *Anal. Chem.* **1987**, *59*, 283-291.
(7) Bowers, C. P.; Fogelman, K. D.; Nagy, J. C.; Ridley, T. Y.; Wang, Y. L.; Evetts, S. W.; Margerum, D. W. To be submitted for publication.
(8) Lister, M. W.; McLeod, P. E. *Can. J. Chem.* **1971**, *49*, 1987-1992.
(9) Simoyi, R. H.; Masvikeni, P.; Sikosana, A. *J. Phys. Chem.* **1986**, *90*, 4126-4131.
(10) Troy, R. C.; Kelley, M. D.; Nagy, J. C.; Margerum, D. W. Submitted for publication in *Inorg. Chem.*
(11) Awtrey, A. D.; Connick, R. E. *J. Am. Chem. Soc.* **1951**, *73*, 1842-1843.
(12) Engel, P.; Oplatka, A.; Perlmutter-Hayman, B. *J. Am. Chem. Soc.* **1954**, *76*, 2010-2015.

0020-1669/91/1330-3538$02.50/0

Ar with an Ascarite vent to prevent significant CO_2 absorption and was standardized by titration against KHP. Sodium iodide solutions were flushed with Ar to remove any dissolved oxygen. The NaI stock solution was stored in the dark and standardized by addition of Br_2 to oxidize I^- to IO_3^-; the resulting solution was then titrated iodometrically with $Na_2S_2O_3$.[13] Sodium sulfite solutions were prepared by dissolution of the weighed solid in an appropriate medium that had been bubbled with Ar for at least 0.5 h. These solutions were used immediately with careful transfer techniques to prevent any O_2 absorption and any metallic contamination. The solutions were standardized by iodometric titration methods.

Methods. UV–vis spectra were recorded on a Perkin-Elmer 320 spectrophotometer. Solution pH values were measured with a Corning Model 476051 combination glass electrode and an Orion Model SA 720 pH meter. Hydrogen ion concentrations were calculated from the pH measurements (p[H^+] = 0.9820pH + 0.252; μ = 0.50 M, 25.0 °C) on the basis of the electrode response to titration of NaOH with $HClO_4$. Gran plots[14] were used to calibrate the electrodes.

A Hi-Tech Scientific Model SFL-43 multimixing module attached by fiber optics to a Durrum D-110 monochromator and interfaced to a Zenith 151 CPU with a Metrabyte DASH-16 A/D converter was used to collect stopped-flow data. A new mixing cell, utilizing a ball mixer and a twin observation path, was used.[15] The total cell path length is 1.60 cm and the dead time for the instrument is 2.7 ms for this mixing/observation cell. The cell design permits first-order rate constants as large as 350 s^{-1} to be measured without correction for mixing effects.[16]

Hydrolysis of $BrSO_3^-$. Bromosulfate was generated within the stopped-flow mixing cell, and its hydrolysis reaction was studied by use of an indicator. First-order rate constants were determined from the absorbance change at 410 nm by analysis of eq 7, where A_∞ is the final

$$\ln\left(\frac{1/A_t - 1/A_\infty}{1/A_0 - 1/A_\infty}\right) = -k_h t \qquad (7)$$

absorbance, A_0 is the initial absorbance, and A_t is the absorbance at any time (t).[4] Rate constants (μ = 0.50 M ($NaClO_4$), 0.0–4.0 °C) are the average of six trials. An aqueous stock solution of 4.16×10^{-4} M 2,4-dinitrophenol (analytical reagent grade; pK_a = 4.11)[17] was prepared, and appropriate dilutions were made in the sulfite solutions to prevent any possible reactions between the indicator and HOBr.

Pulsed-Accelerated-Flow Method. A pulsed-accelerated-flow spectrometer, Model IV,[3,7] was used to obtain kinetic data for the reactions of iodide and sulfite with hypobromite. This instrument has a wavelength range of 200–850 nm, and improvements in the optics lead to much higher light throughput as compared with that of earlier models.[5,6] The PAF spectrometer employs integrating observation[18,19] during continuous-flow mixing of short duration (a 0.4-s pulse). The purpose of the pulsed flow is to conserve reagents.[5,6] The reactants are observed along the direction of flow from their point of mixing to their exit from the observation tube (1.025 cm). A twin-path mixing/observation cell made from poly(vinyl chloride) is used.[6] In this study, the flow was decelerated during the pulse to give a linear velocity ramp, and 250 measurements of the transmittance were taken as the flow velocity in the observation tube changed from 12.5 to 3.0 m s^{-1}. The velocity variation permits the chemical reaction rate process to be resolved from the mixing rate process. The method of observation, the efficient mixing, and the variation of flow velocity permit accurate measurement of first-order rate constants that are factors of 10^3 larger than can be measured by typical stopped-flow methods. Solution reservoirs, drive syringes, and the mixing/observation cell were thermostated at 25.0 (±0.2) °C with a circulating water bath. Reactant solutions were drawn directly from the reservoirs into the drive syringes through Teflon tubing.

Equation 8 is used in the analysis of PAF data under pseudo-first-order conditions,[6] where M_{exp} is the defined absorbance ratio, A_v is the

$$M_{exp} = \frac{A_v - A_\infty}{A_0 - A_\infty} = \frac{1}{bk_m} + \frac{v}{bk_r} \qquad (8)$$

absorbance of the reaction mixture at a given instantaneous velocity, A_∞ is the absorbance at infinite time, A_0 is the absorbance at time zero, k_r is the reaction rate constant (s^{-1}), b is the reaction path length (0.010 25 m), v is the solution velocity in the observation tube (m s^{-1}), and k_m is a proportionality constant from the mixing rate constant (k_{mix}) where $k_m = k_{mix}/v$. Linear plots of M_{exp} vs v have slopes of $1/(bk_r)$ for first-order reactions.

The reactions of OBr^- with SO_3^{2-} are so fast that second-order unequal-concentration conditions are needed. Equation 9 gives the relationship[19] for the M_{exp} values where A_a and C_a equal the absorbance and concentration of the excess reagent, A_b and C_b equal the absorbance and concentration of the limiting reagent, A_p equals the absorbance of the products, d is the cell path length, and q equals C_b/C_a. The apparent rate constant (k_{app}) is related to the reaction rate constant (k_r) and the mixing rate constant (k_{mix}) by eq 10. Gerritsen and Margerum[20] have

$$M_{exp} = \frac{A_v - A_a(1-q) - A_p}{A_a + 1/q(A_b - A_p)} = \frac{1-q}{R}\ln\left(\frac{1-qe^{-R}}{1-q}\right) \qquad (9)$$

$$R = \frac{k_{app}C_a d(1-q)}{v}$$

$$\frac{1}{k_{app}} = \frac{1}{k_{mix}} + \frac{1}{k_r} \qquad (10)$$

shown that when $qe^{-R} \ll 1$, k_r can be solved for directly by using eq 11,

$$M_{exp} = \frac{1}{k_m C_a d}\ln\left(\frac{1}{1-q}\right) + \frac{v}{k_r C_a d}\ln\left(\frac{1}{1-q}\right) + \frac{c}{v} \qquad (11)$$

where c is a constant that originates from the mixing behavior in the center of the twin-path cell. Inclusion of a c/v term is also needed in the analysis procedure used[7] for first-order rate constants greater than 10^5 s^{-1}. Equation 11 is solved by linear regression to give the best fit of k_m, k_r, and c. All of the k_r values determined in the $OBr^- + SO_3^{2-}$ study meet the condition $qe^{-R} \ll 1$, so that analysis by this simplification is appropriate.

Kinetic data obtained on the PAF spectrometer were collected at μ = 0.50 M ($NaClO_4$/NaOH) and 25.0 °C by following the disappearance of OBr^- at 329 nm. Data for I^- reactions were corrected for light scattering due to small refractive index differences between the iodide ion solutions and the corresponding $NaClO_4$/NaOH solutions without I^- present. The absorbance change due to refractive index differences decreases as the velocity increases, because the light scattering is diminished as the mixing rate constant increases. The absorbance changes due to scattering are subtracted from the reaction absorbance data, which are then analyzed in the usual manner. The k_r values reported in the tables are an average of three or four trials. The values in parentheses denote one standard deviation in the last digit.

Results and Discussion

Acid Dissociation Constant of HOBr. The K_a value for HOBr at 25.0 °C and μ = 0.50 M was not available, so we evaluated the constant under these conditions. Nine solutions of OBr^- ($[OBr]_T = 5.0 \times 10^{-4}$ M, $[OBr]_T = [OBr^-] + [HOBr]$) were prepared from p[$H^+$] = 5.04 to 10.73, and the absorbance was measured at 300 nm (ϵ_{OBr^-} = 150 M^{-1} cm^{-1}; ϵ_{HOBr} = 50 M^{-1} cm^{-1}).[21] These data were used to calculate a pK_a value for HOBr from eq 12, where A_{max} = absorbance when only OBr^- contributes,

$$pK_a = -\log[H^+] + \frac{A_{max} - A_{pH}}{A_{pH} - A_{min}} \qquad (12)$$

A_{pH} = absorbance when both OBr^- and HOBr contribute, and A_{min} = absorbance when only HOBr contributes to the total absorbance. The pK_a value determined by this method is 8.8 ± 0.1. It is in good agreement with other reported values at unspecified ionic strengths. Farkas and Lewin[22] found pK_a = 8.70 at 25 °C. Shilov[23] used electrochemical titrations to determine a pK_a = 8.7 at 20 °C. These studies did not specify the ionic strength or the precision of the values.

Kinetics of the Hypobromite Reaction with Iodide. Excellent linear plots of M_{exp} against velocity (eq 8) are obtained for the reaction of OBr^- with I^- by use of the PAF method. The loss of OBr^- is observed (ϵ = 345 M^{-1} cm^{-1} at 329 nm), and the final product is OI^- (ϵ = 30 M^{-1} cm^{-1} at 329 nm). Neither I^- nor Br^- has any absorbance at this wavelength. The resulting pseudo-

(13) Kolthoff, I. M.; Sandell, E. B.; Meehan, E. J.; Bruckenstein, S. *Quantitative Chemical Analysis*, 4th ed.; Macmillan: London, 1969; p 852.
(14) Rossotti, F. J. C.; Rossotti, H. *J. Chem. Educ.* **1965**, *42*, 375–378.
(15) Wang, Y. L. Ph.D. Thesis, Purdue University, 1989.
(16) Dickson, P. N.; Margerum, D. W. *Anal. Chem.* **1986**, *58*, 3153–3158.
(17) Kolthoff, I. M. *J. Phys. Chem.* **1930**, *34*, 1466–1483.
(18) Gerischer, H.; Heim, W. *Z. Phys. Chem. (Munich)* **1965**, *46*, 345–352.
(19) Gerischer, H.; Heim, W. *Ber. Bunsen-Ges. Phys. Chem.* **1967**, *71*, 1040–1046.
(20) Gerritsen, C. M.; Margerum, D. W. To be submitted for publication.
(21) Galal-Gorchev, H.; Morris, J. C. *Inorg. Chem.* **1965**, *4*, 899–905.
(22) Farkas, L.; Lewin, M. *J. Am. Chem. Soc.* **1950**, *72*, 5766–5767.
(23) Shilov, E. *J. Am. Chem. Soc.* **1938**, *60*, 490–492.

Table I. Pseudo-First-Order Rate Constants for the OBr^- Reaction with I^- from PAF Measurements[a]

$[OH^-]$, M	$10^3[I^-]$, M	$10^{-3}k_r$, s^{-1}	$[OH^-]$, M	$10^3[I^-]$, M	$10^{-3}k_r$, s^{-1}
0.100	5.00	6.3 (2)	0.100	10.0	12.9 (4)
0.100	6.25	8.0 (2)	0.200	7.50	7.01 (9)
0.100	7.50	9.6 (2)	0.350	7.50	6.46 (8)
0.100	8.75	11.4 (4)	0.500	7.50	5.93 (9)

[a] Conditions: $[OBr^-] = 4.0 \times 10^{-4}$ M; $\lambda = 329$ nm; 25.0 °C, $\mu = 0.50$ M ($NaOH/NaClO_4$).

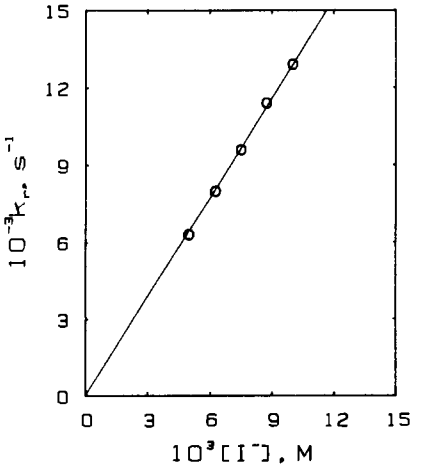

Figure 1. Iodide dependence of the pseudo-first-order rate constant (k_r) for the reaction of OBr^- (4.0×10^{-4} M) with iodide in 0.100 M OH^- (25.0 °C, $\mu = 0.50$ M).

first-order rate constants vary from 5930 to 12900 s^{-1} and are summarized in Table I. Figure 1 shows that k_r varies linearly with $[I^-]$ (at constant $[OH^-] = 0.10$ M) and that the intercept is zero. The slope is 1.29 (±0.01) × 10^6 M^{-1} s^{-1}. A plot of k_r against $1/[OH^-]$ at constant $[I^-]$ is shown in Figure 2, where the slope is 450 (±30) M s^{-1} and the intercept is 5.0 (±0.1) × 10^3 s^{-1}. The inverse dependence in hydroxide concentration indicates that HOBr is more reactive than OBr^- with I^-, as is the case[1,2] for the I^- reaction with HOCl and OCl^-. The rate expression is given by eq 13, where k_0 is 6.8 (±0.4) × 10^5 M^{-1} s^{-1}, $K_1 = K_w/K_a$

$$\frac{-d[OBr^-]}{dt} = \left(k_0 + \frac{K_1 k_2}{[OH^-]}\right)[I^-][OBr^-] \qquad (13)$$

= 1.2×10^{-5} M ($pK_w = 13.73$ at $\mu = 0.5$ M, 25.0 °C),[24] and k_2 is 5.0 (±0.3) × 10^9 M^{-1} s^{-1}.

The proposed mechanism is given by eqs 14–19, where IBr(aq) is a common intermediate for both the OBr^- and the HOBr reactions. Rate equations for the aqueous hydrolysis ($k^{IBr}_{H_2O}$ =

$$H_2O + OBr^- + I^- \xrightarrow{k_0} 2OH^- + IBr(aq) \qquad (14)$$

$$OBr^- + H_2O \underset{k_{-1}}{\overset{k_1}{\rightleftharpoons}} HOBr + OH^- \qquad (15)$$

$$HOBr + I^- \xrightarrow{k_2} OH^- + IBr(aq) \qquad (16)$$

$$IBr(aq) + H_2O \xrightarrow{k^{IBr}_{H_2O}} HOI + Br^- + H^+ \qquad (17)$$

$$IBr(aq) + OH^- \xrightarrow{k^{IBr}_{OH}} HOI + Br^- \qquad (18)$$

$$HOI + OH^- \xrightarrow{k^{HOI}_{OH}} OI^- + H_2O \qquad (19)$$

8×10^5 s^{-1}) and base hydrolysis ($k^{IBr}_{OH} = 6.0 \times 10^9$ M^{-1} s^{-1}) of IBr(aq)[10] are much larger than the observed k_r values. Therefore IBr(aq) is rapidly converted to HOI, which in turn rapidly forms

(24) Langerstrom, G. *Acta Chem. Scand.* **1959**, *13*, 722–736.

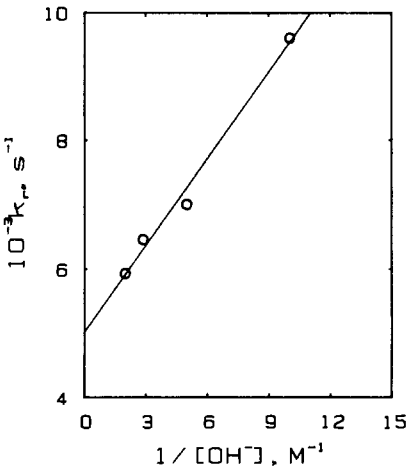

Figure 2. Hydroxide dependence of the pseudo-first-order rate constant (k_r) for the reaction of OBr^- (4.0×10^{-4} M) with iodide (7.50×10^{-3} M) at 25.0 °C and $\mu = 0.50$ M.

OI^- ($k^{HOI}_{OH} \simeq 10^{10}$ M^{-1} s^{-1}). Hence, the observed stoichiometric reaction is given by eq 20. However, direct attack of I^- on oxygen

$$OBr^- + I^- \rightarrow OI^- + Br^- \qquad (20)$$

is unlikely for such fast reactions because it is difficult to expand the coordination number of oxygen. On the other hand, the much larger rate constant for $OBr^- + I^-$ (6.8×10^5 M^{-1} s^{-1}) compared to that for $OCl^- + I^-$ (<30 M^{-1} s^{-1})[24] is consistent with I^- attack at bromine because of the relative ease of expanding the coordination around bromine compared to chlorine.

The rate expression in eq 13 requires that a preequilibrium condition exist between OBr^- and HOBr (eq 15). The specific steady-state requirement is that $k_{-1}[OH^-] \gg k_2[I^-]$. This is valid because the lowest $[OH^-]$ is 0.10 M and the highest $[I^-]$ is 0.010 M, while $k_{-1} \simeq 10^{10}$ M^{-1} s^{-1} and $k_2 = 5 \times 10^9$ M^{-1} s^{-1}.

In the reactions of HOCl with I^- in acid, kinetic evidence was found for small concentrations of a $HOClI^-$ intermediate.[2] This type of intermediate should be easier to form with $HOBrI^-$ (structure I), because of more favorable soft–soft interactions[25-28]

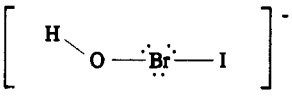

I

as well as the enhanced ability to have 10 electrons around bromine compared to chlorine. However, the reactions are studied in strong base, so that there are always negligible concentrations of HOBr as well as $HOBrI^-$. The rapid loss of OH^- from this intermediate yields IBr(aq) (eq 16). We propose a similar intermediate in the reaction of OBr^- with I^- and a water molecule (eq 21). The rate

$$H_2O + OBr^- + I^- \underset{k_{-a}}{\overset{k_a}{\rightleftharpoons}} OH^- + HOBrI^- \xrightarrow{k_b} 2OH^- + BrI \qquad (21)$$

constant, k_b, for loss of OH^- from $HOBrI^-$, must be very large because the inequality $k_b \gg k_{-a}[OH^-]$ is needed to avoid hydroxide suppression of this pathway. Alternatively, a transition state could exist (structure II) where two bonds must be broken (O–H from

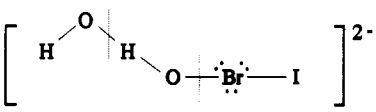

II

H_2O and O–Br from OBr^-) as a Br–I bond forms, so that 2 OH^- and IBr are formed.

(25) Gerritsen, C. M.; Margerum, D. W. *Inorg. Chem.* **1990**, *29*, 2757–2762.
(26) Pearson, R. G. *Proc. Natl. Acad. Sci. U.S.A.* **1986**, *83*, 8440–8441.
(27) Klopman, G. *J. Am. Chem. Soc.* **1968**, *90*, 223–234.
(28) Pearson, R. G. *Inorg. Chem.* **1988**, *27*, 734–740.

Table II. Summary of Rate Constants for the Reaction of Hypobromite with Excess Iodide in Base

reaction	k_f[a]	k_r[a]	ref
$H_2O + OBr^- + I^- \rightarrow IBr + 2OH^-$	6.8×10^5		*b*
$OBr^- + H_2O \rightleftharpoons HOBr + OH^-$	1.2×10^5	10^{10}	*c*
$HOBr + I^- \rightarrow IBr + OH^-$	5.0×10^9		*b*
$IBr + OH^- \rightarrow HOI + Br^-$	6×10^9		*d*
$IBr + H_2O \rightarrow HOI + Br^- + H^+$	8×10^5		*d*
$IBr + I^- \rightarrow I_2 + Br^-$	2.1×10^9		*d*
$HOI + OH^- \rightleftharpoons OI^- + H_2O$	10^{10}	8×10^6	*c*
$HOI + I^- \rightleftharpoons I_2OH^-$	6.7×10^5	994	19
$I_2OH^- \rightleftharpoons I_2 + OH^-$	3×10^5	10^{10}	19
$I_2 + I^- \rightleftharpoons I_3^-$	6×10^9	8×10^6	*e*

[a] All concentrations in molarity; times in seconds. [b] This study. [c] Estimated from the pK_a of the acid and pK_w[24] (pK_a for HOI is 10.6: Chia, Y. T. *U.S. Energy Commun., UCRL*-8311 **1958**). [d] Troy, R. C.; Kelley, M. D.; Nagy, J. C.; Margerum, D. W. To be submitted for publication. [e] Turner, D. H.; Flynn, G. W.; Sutin, N.; Beitz, J. V. *J. Am. Chem. Soc.* **1972**, *94*, 1554–1559.

Table III. Rate Constants for the Reaction of Hypobromite with Sulfite[a]

$10^4[OBr^-]$, M	$10^4[SO_3^{2-}]$, M	$[OH^-]$, M	$10^{-8}k_{obsd}$, M^{-1} s^{-1}
3.81	6.29	0.5	1.1 (3)
3.81	7.96	0.5	1.2 (1)
3.81	9.57	0.5	0.9 (1)
3.75	8.05	9.1×10^{-3}	0.9 (1)
4.46	8.27	3.9×10^{-4}	2.6 (1)[b]
3.85	9.02	1.6×10^{-4}	4.8 (9)[b]

[a] Conditions: PAF measurements with second-order unequal concentrations, 25.0 °C, μ = 0.50 M, λ = 329 nm. [b] $[CO_3]_T = [HCO_3^-] + [CO_3^{2-}]$ = 0.10 M.

Interference from I_2OH^- and I_3^-. If the hydroxide concentration is substantially less than 0.1 M, additional reactions interfere in studies of the OBr^- and I^- reaction kinetics. The molar absorptivity of I_3^- is very large at 329 nm (ϵ = 17 400 M^{-1} cm^{-1}), so trace levels (10^{-6} M) of this species will contribute to the absorbance of the products. In addition to the reactions in eqs 14–19, there are competitive reactions between I^- and OH^- with IBr(aq) and between HOI, I_2, I_2OH^-, and I_3^- that become important as $[OH^-]$ is decreased (Table II). Some of the reactions are on the same time scale as the $OBr^- + I^-$ reactions and can confuse the PAF measurements. An ACCUCHEM program[29] was used to calculate concentration versus time profiles for all the species and reactions in Table II. The results show no interference in the absorbance measurements from I_3^- or other species if $[OH^-] \geq 0.1$ M when $[I^-] = 0.005$–0.010 M. The correct value of A_∞ is very important in the PAF measurements, because this value must correspond to the end of the fast reaction under study as opposed to a subsequent slower reaction. This is of concern because of necessary time delays (~20 s) when the A_∞ value is measured by pulling the completely mixed system back into the PAF observation tube. Separate reactions were mixed by stopped-flow methods in order to be able to measure A_∞ within 4 ms. Under the specified conditions, the two A_∞ values are in agreement. Thus, the disproportionation reactions of OI^- (to give IO_3^- and I^-) are too slow[30,31] to shift the A_∞ values.

Kinetics of the Hypobromite Reaction with Sulfite. Even with 0.5 M OH^- concentrations, the reaction of OBr^- with SO_3^{2-} is so fast that it is difficult to use excess SO_3^{2-} concentrations for pseudo-first-order PAF kinetics. Therefore, the reactions are monitored by the loss of OBr^- under second-order unequal-concentration conditions with initial SO_3^{2-} to OBr^- ratios of 1.6–2.5 (Table III). All trials give excellent fits for eq 11. The average value of the observed second-order rate constants is 1.0 (±0.1) $\times 10^8$ M^{-1} s^{-1}, and the rate constants are independent of hydroxide ion concentration from 0.50 to 0.0091 M OH^-. As $[OH^-]$ is lowered to 1.6×10^{-4} M, the k_{obsd} value increases to 4.8 (±0.9) $\times 10^8$ M^{-1} s^{-1}. The reaction time is so short under these conditions (first half-life = 2.8 μs) that we are near the limit of the PAF measurements.

A mechanism analogous to that for OBr^- and I^- is given in eqs 22–25, where Br^+ transfer gives $BrSO_3^-$ as the initial product.

$$H_2O + OBr^- + SO_3^{2-} \xrightarrow{k_3} BrSO_3^- + 2OH^- \quad (22)$$

$$OBr^- + H_2O \underset{k_{-1}}{\overset{k_1}{\rightleftharpoons}} HOBr + OH^- \quad (23)$$

$$HOBr + SO_3^{2-} \xrightarrow{k_4} BrSO_3^- + OH^- \quad (24)$$

$$BrSO_3^- + H_2O \rightarrow SO_4^{2-} + Br^- + 2H^+ \quad (25)$$

The rate expression for eqs 22–24 would be given by eq 26 if HOBr and OBr^- were in rapid equilibrium. This expression takes into

$$\frac{-d[OBr^-]_T}{dt} = \left(\frac{k_3[OH^-] + K_1k_4}{K_1 + [OH^-]}\right)[SO_3^{2-}][OBr^-]_T \quad (26)$$

account the appreciable concentration of HOBr at the lowest $[OH^-]$ values ($[OBr^-]_T = [OBr^-] + [HOBr]$). Since k_3 is 1.0×10^8 M^{-1} s^{-1} and K_1 is 1.2×10^5 M, we can evaluate k_4 as 5 (±1) $\times 10^9$ M^{-1} s^{-1}, which equals or very nearly equals the diffusion limit. A new problem now appears to exist, because the prior equilibrium condition for HOBr requires $k_{-1}[OH^-] > k_4[SO_3^{2-}]$. A typical value for k_{-1} is 10^{10} M^{-1} s^{-1}, so when $[OH^-] = 1.6 \times 10^{-4}$ M, the $k_{-1}[OH^-]$ value is 1.6×10^6 s^{-1}, while for $[SO_3^{2-}] = 9.0 \times 10^{-4}$ M the $k_4[SO_3^{2-}]$ product is 4.5×10^6 s^{-1} and the inequality does not hold. In other words, the proton-transfer step from H_2O to OBr^- is too slow to permit the HOBr path. This problem is avoided by the use of 0.1 M concentrations of carbonate buffer, so that rapid proton transfer is provided by the reactions in eq 27. The pK_a value for HCO_3^- is 9.7 compared to 8.8 for

$$HCO_3^- + OBr^- \underset{k'_{-1}}{\overset{k'_1}{\rightleftharpoons}} HOBr + CO_3^{2-} \quad (27)$$

HOBr, so $k'_1/k'_{-1} = 0.13$. We can estimate k'_{-1} to be 3×10^8 M^{-1} s^{-1} from comparable rate constants for $CO_3^{2-} + HOCl$ and the relative ΔpK_a values.[3,32] The new inequality condition for preequilibrium of OBr^- and HOBr is now $(k_{-1}[OH^-] + k'_{-1}[CO_3^{2-}]) > k_4[SO_3^{2-}]$. Under our conditions for the lowest $[OH^-]$ used, the first two terms are a factor of 7 larger than $k_4[SO_3^{2-}]$ at the start of the reaction and a factor of 12 larger near the end of the reaction. Thus, it is valid, within our experimental error, to assume that HOBr and OBr^- are in equilibrium because of the presence of carbonate buffer.

In the reaction of HOCl with SO_3^{2-}, kinetic evidence was found[3] for a reactive intermediate, $HOClSO_3^{2-}$, where HCO_3^- assists its breakup (eqs 28 and 29). We expect HOBr to form a similar

$$HOClSO_3^{2-} \rightarrow OH^- + ClSO_3^- \quad (28)$$

$$HOClSO_3^{2-} + HCO_3^- \rightarrow H_2O + ClSO_3^- + CO_3^{2-} \quad (29)$$

intermediate, $HOBrSO_3^{2-}$, but it must dissociate more easily than $HOClSO_3^{2-}$ because the k_4 value for eq 24 is 5×10^9 M^{-1} s^{-1} compared to a value of 7.6×10^8 M^{-1} s^{-1} for the corresponding reaction between HOCl and SO_3^{2-}. A more reactive $HOBrSO_3^{2-}$ species is expected because the O–Br bond is weaker than the O–Cl bond.[33] Thus, the reaction in eq 24 is at the diffusion limit and HCO_3^- assistance for the breakup of $HOBrSO_3^{2-}$ is not needed.

Hydrolysis of the Bromosulfate Ion. Evidence for the formation of $BrSO_3^-$ is provided by rapid stopped-flow mixing of HOBr and SO_3^{2-} in the presence of an indicator. If the reaction took place by oxygen atom transfer, a one-step process (eq 30) with im-

$$HOBr + SO_3^{2-} \rightarrow Br^- + SO_4^{2-} + H^+ \quad (30)$$

(29) Braun, W.; Herron, J. T. *ACCUCHEM*; National Bureau of Standards: Gaithersburg, MD, 1988.
(30) Thomas, T. R.; Pence, D. T.; Hasty, R. A. *J. Inorg. Nucl. Chem.* **1980**, *42*, 183–186.
(31) Wren, J. C.; Paquette, J.; Sunder, S.; Ford, B. L. *Can. J. Chem.* **1986**, *64*, 2284–2296.
(32) Eigen, M. *Angew. Chem., Int. Ed. Engl.* **1964**, *3*, 1–72.
(33) Darwent, B. deB. *Natl. Stand. Ref. Data Ser.* (*U.S. Natl. Bur. Stand.*) **1970**, *31*, 17, 26.

Table IV. First-Order Rate Constants for the Hydrolysis Reaction of Bromosulfate Ion[a]

T, K	k_h, s^{-1}
273.0[b]	230 (20)
275.0[c]	290 (40)
277.0[b]	360 (40)

[a] Conditions: stopped-flow indicator method; μ = 0.50 M ($NaClO_4$), λ = 410 nm; [2,4-dinitrophenol] = 2.2×10^{-5} M. [b] [HOBr] = 5.0×10^{-4} M (p[H^+] = 6.63); $[SO_3]_T = [HSO_3^-] + [SO_3^{2-}] = 5.3 \times 10^{-4}$ M (p[H^+] = 6.71). [c] [HOBr] = 5.0×10^{-4} M (p[H^+] = 6.65); $[SO_3]_T = 5.0 \times 10^{-4}$ M (p[H^+] = 6.83). Final p[H^+] after mixing is 3.39.

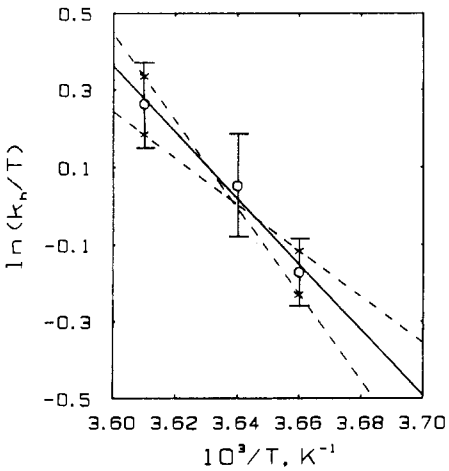

Figure 3. Eyring plot for the temperature dependence of k_h for the hydrolysis of $BrSO_3^-$. The vertical bars show the standard deviation of the k_h values at each temperature. The dashed lines show the extreme slopes possible for the probable error range at 0.0 and 4.0 °C (marked by ×). The linear least-squares slope and intercept give $\Delta H^\ddagger = 70 \pm 8$ kJ mol^{-1} and $\Delta S^\ddagger = 60 \pm 8$ J mol^{-1} K^{-1}, while the extreme slopes give uncertainties of ±20 kJ mol^{-1} for $\Delta H^\ddagger$ and ±80 J mol^{-1} K^{-1} for $\Delta S^\ddagger$.

mediate release of acid would be expected. The PAF experiments show that this would occur within the mixing time of the stopped-flow instrument. On the other hand, a Br^+-transfer reaction should occur in two steps (eqs 31 and 32) with the fast release

$$HOBr + SO_3^{2-} \rightarrow OH^- + BrSO_3^- \quad (31)$$

$$BrSO_3^- + H_2O \xrightarrow{k_h} Br^- + SO_4^{2-} + 2H^+ \quad (32)$$

of base, and the slower release of acid as is observed in the case of the formation and decay of $ClSO_3^-$. The rate of hydrolysis of $BrSO_3^-$ is faster than the rate hydrolysis of $ClSO_3^-$, but we are able to observe the reaction in eq 32 by the change in absorbance of an indicator (2,4-dinitrophenol) at 0–4 °C (Table IV). The magnitude of the rate constants and the freezing point of the solvent severely limit the range of temperature that can be studied by the stopped-flow method. At 0.0 °C the k_h value is 230 (±20) s^{-1}. Figure 3 shows a linear least-squares fit of ln (k_h/T) vs $1/T$ that gives $\Delta H^\ddagger = 70 \pm 8$ kJ mol^{-1} and $\Delta S^\ddagger = 60 \pm 8$ J mol^{-1} s^{-1}. The plot includes the standard deviation of six measurements of the k_h value at each temperature. In order to indicate the considerable degree of uncertainty that is associated with the slope and intercept measurements over this narrow temperature range, we show two slopes (dashed lines) that would result from selection of the extremes of the probable error (0.6745σ) for the 0 and 4 °C data. These slopes give a much wider uncertainty than the linear least-squares values and correspond to $\Delta H^\ddagger = 70$ (±20) kJ mol^{-1} and $\Delta S^\ddagger = 60$ (±80) J mol^{-1} K^{-1}.

Comparison of Halosulfate Hydrolysis Kinetics. At 2.0 °C the hydrolysis rate constants are in the following order: $BrSO_3^-$ (290 s^{-1}) ≫ $ClSO_3^-$ (48 s^{-1})[4] > ISO_3^- (32 s^{-1}).[34] Each of these halosulfate ions was formed by X^+-transfer reactions with SO_3^{2-} (from HOBr, HOCl, and I_2, respectively). In contrast to these relatively rapid hydrolysis reactions, FSO_3^- hydrolysis is extremely slow.[35] Table V compares the k_h values at 25 °C and the activation parameters for four halosulfate ions. (The fluorosulfate hydrolysis reaction is faster in high acid and high base concentrations, but the water hydrolysis path predominates from pH 3 to pH 12.[35] The hydrolysis rate constants for the other halosulfate ions are all measured from pH 3 to pH 7, so only the water path is considered.) The necessity to extrapolate the hydrolysis rate constant for $BrSO_3^-$ from 0–4 to 25 °C means that the value of 3×10^3 s^{-1} has a large uncertainty. However, it is clear that the relative rate constants are in the order $BrSO_3^- \gg ISO_3^- \simeq ClSO_3^- \gg FSO_3^-$. The very small rate constant for the hydrolysis of FSO_3^- is associated with the large negative activation entropy for this reaction. The activated state must have a high degree of F^- aquation. Table VI gives $\Delta H°$ and $\Delta S°$ values calculated for the hydration of the gaseous halide ions. It is of interest to compare the change of $\Delta S^\ddagger$ values from FSO_3^- to ISO_3^-, where $\Delta(\Delta S^\ddagger)$ is +146 J mol^{-1} K^{-1}, to the corresponding change of $\Delta S°$ values from F^- to I^-, where $\Delta(\Delta S°)$ is +98 J mol^{-1} K^{-1}. This suggests that the relative decrease in solvent organization around the halide ions in going from F^- to I^- plays an important role in the relative rate of hydrolysis of the halosulfate ions. The large changes in the $\Delta H°$ values for the aquation of the halide ions are offset by changes in the X–S bond strength, so that changes in $\Delta H^\ddagger$ values are relatively small in comparison to the $>10^{10}$ change in rate constants for the halosulfate hydrolysis reactions. The reasons for the larger rate constants for the hydrolysis of $BrSO_3^-$ compared to $ClSO_3^-$ and ISO_3^- are not clear. The uncertainties in the $\Delta H^\ddagger$ and $\Delta S^\ddagger$ values for $BrSO_3^-$ are too great to permit interpretation

Table V. Halosulfate Hydrolysis Rate Constants (25 °C) and Activation Parameters

species	k_h, s^{-1}	$\Delta H^\ddagger$, kJ mol^{-1}	$\Delta S^\ddagger$, J mol^{-1} K^{-1}	ref
FSO_3^-	3.1×10^{-7}	73[a]	−125	35
$ClSO_3^-$	270	49	−32	4
$BrSO_3^-$	3×10^3[b]	70 ± 20	60 ± 80	this work
ISO_3^-	298	65	21	34

[a] Calculated from k_h and $\Delta S^\ddagger$. [b] Calculated from k_h at 2 °C and $\Delta H^\ddagger$ = 70 kJ mol^{-1}.

Table VI. Enthalpies and Entropies for the Hydration of Gaseous Halide Ions[a]

	$\Delta H°$, kJ mol^{-1} [b,c]	$\Delta S°$, J mol^{-1} K^{-1} [d,e]		$\Delta H°$, kJ mol^{-1} [b,c]	$\Delta S°$, J mol^{-1} K^{-1} [d,e]
F^-	−515	−160	Br^-	−347	−81
Cl^-	−381	−96	I^-	−305	−62

[a] $X^-(g) + H_2O \rightarrow X^-(aq)$. [b] Cotton, F. A.; Wilkinson, G. *Advanced Inorganic Chemistry*; Wiley: New York, 1980; p 66. [c] Halliwell, H. F.; Nyburg, S. C. *Trans. Faraday Soc.* **1963**, *59*, 1126–1140. [d] *Standard Potentials in Aqueous Solution*; Bard, A. J., Parsons, R., Jordan, J., Eds.; Dekker: New York, 1985; pp 67–90. [e] *JANAF Thermochemical Tables*, 3rd ed.; Chase, M. W., Jr., Ed.; American Chemical Society and American Institute of Physics: New York, 1986.

Table VII. Rate Constants for Hypohalite and Hypohalous Acid Reactions with Iodide and with Sulfite[a]

reaction	k, M^{-1} s^{-1}	ref
$H_2O + OCl^- + I^- \rightarrow ICl + 2OH^-$	<30	25, *b*
$H_2O + OBr^- + I^- \rightarrow IBr + 2OH^-$	6.8×10^5	this study
$HOCl + I^- \rightarrow ICl + OH^-$	1.4×10^8	1
$HOBr + I^- \rightarrow IBr + OH^-$	5.0×10^9	this study
$H_2O + OCl^- + SO_3^{2-} \rightarrow ClSO_3^- + 2OH^-$	2.3×10^4	3
$H_2O + OBr^- + SO_3^{2-} \rightarrow BrSO_3^- + 2OH^-$	1.0×10^8	this study
$HOCl + SO_3^{2-} \rightarrow ClSO_3^- + OH^-$	7.6×10^8	3
$HOBr + SO_3^{2-} \rightarrow BrSO_3^- + OH^-$	5.0×10^9	this study

[a] Conditions: 25.0 °C, μ = 0.50 M. [b] Kumar, K.; Margerum, D. W. Unpublished data.

(34) Yiin, B. S.; Margerum, D. W. *Inorg. Chem.* **1990**, *29*, 1559–1564.

(35) Jones, M. M.; Lockhart, W. L. *J. Inorg. Nucl. Chem.* **1968**, *30*, 1237–1243.

in terms of the nature of the transition state.

Conclusions

Rate constants for the hypohalite and hypohalous acid reactions with iodide and sulfite ions are summarized in Table VII. The OBr^- reactions are faster than the OCl^- reactions by a factor of more than 2.3×10^4 for I^- and by a factor of 4.4×10^3 for SO_3^{2-}. We propose that these enhanced rates are associated with the greater ease of Br^+-transfer compared to Cl^+-transfer reactions. In other words, nucleophilic attack at bromine with expansion of its valence-shell electrons is more favorable than the corresponding attack at chlorine. The reactivity of HOBr is much greater than that of OBr^- (by a factor of 7.4×10^3 for I^- and a factor of 50 for SO_3^{2-}). The HOBr reactions with I^- and with SO_3^{2-} are so favorable that the rate constants reach the diffusion limit. The high reactivity of HOBr is again associated with the greater ease of Br^+ transfer to the nucleophiles (I^- or SO_3^{2-}) accompanied by the rapid loss of OH^-. The indicator experiments provide evidence for the formation and decay of $BrSO_3^-$.

Acknowledgment. Support for this work was provided by National Science Foundation Grant CHE-8720318. R.C.T. also wishes to thank the Dow Chemical Co. for a 1989 Summer Fellowship.

Registry No. OBr^-, 14380-62-2; I^-, 20461-54-5; SO_3^{2-}, 14265-45-3; HOBr, 13517-11-8; $BrSO_3^-$, 44047-97-4.

Contribution from the Departments of Chemistry, University of Nottingham, Nottingham NG7 2RD, U.K., and University Center at Binghamton, State University of New York, P.O. Box 6000, Binghamton, New York 13902-6000

Time-Resolved Infrared Spectrum of the MLCT Excited State of $W(CO)_5$(4-CNpyr) (4-CNpyr = 4-Cyanopyridine): Photophysics and Photochemistry

Paul Glyn,[†] Frank P. A. Johnson,[†] Michael W. George,[†] Alistair J. Lees,[‡] and James J. Turner*[,†]

Received December 17, 1990

Fast time-resolved infrared spectroscopy is employed to probe the lower metal to 4-CNpyr charge-transfer (MLCT) excited state of $W(CO)_5$(4-CNpyr) (4-CNpyr = 4-cyanopyridine). On visible irradiation, the CO stretching vibrations shift to higher frequency, confirming that in this excited state the metal center is oxidized. The excited state decays back to the ground state and, via the LF excited state, decomposes to $W(CO)_5$ and 4-CNpyr. The rate constants for these processes are equal (ca. 4×10^6 s^{-1}), suggesting that there is a rapid equilibrium between the MLCT and LF states.

Introduction

The photochemistry of $(CO)_5ML$ species has been extensively investigated.[1-4] Low-temperature studies[1] showed that if L is an electron-withdrawing group then the MLCT state is lower than the LF excited states. Lees and Adamson[5] were the first to observe room-temperature emission from such systems. From very detailed studies[6-8] of the photochemistry and photophysics of $(CO)_5WL$, the following conclusions may be drawn in the case of L = 4-CNpyr.

(i) Irrespective of irradiation wavelength, multiple emission occurs from two ^{3}MLCT states,[9] separated by 990 cm^{-1}, in rapid thermal equilibrium with each other. In methylcyclohexane at 296 K, the emissions are centered at 545 and 613 nm and the lifetime is 0.292×10^{-6} s—see Figure 1.

(ii) Immediately following the laser flash, an absorption band with a maximum at ca. 400 nm was observed;[6] this was assigned to the excited state. The decay of this band followed a single exponential with a rate equal to the rate of decay of the emission.

(iii) Substitution photochemistry proceeds from a ^{3}LF state[9] that is some 2600 cm^{-1} above the lower ^{3}MLCT state, and is in steady-state thermal equilibrium with the emitting CT states; the first step involves ejection of 4-CNpyr.

The value of probing excited states of organometallics with resonance Raman spectroscopy[10-12] has already been demonstrated. We recently obtained the IR spectrum of the emitting excited state of $ClRe(CO)_3(4,4'\text{-bpy})_2$ and confirmed from the shift in ν(CO) frequencies that there is charge transfer from metal to the bpy ligand.[13] For $ClRe(CO)_3(4,4'\text{-bpy})_2$, the quantum yield for photodissociation is nearly zero. In this paper, we describe an investigation of $(CO)_5W$(4-CNpyr) and report the ν(CO) IR spectra of the photochemically active ^{3}MLCT excited state, its decay back to the ground state, *and* the dissociation via the excited ^{3}LF state to $W(CO)_5$ and 4-CNpyr.

Table I. Frequencies (cm^{-1}) and Assignment, Based on C_{4v} Symmetry, in the ν(CO) Region of Species Involved in Photochemistry of $W(CO)_5$(4-CNpyr) in Methylcyclohexane

	a_1	e	a_1
$W(CO)_5$(4-CNpyr)[a]	2072.5	1936.4	1929.5 (sh)
$[W(CO)_5$(4-CNpyr)]*	b	2000	1966
$W(CO)_5$··solvent	b	1954	c
$W(CO)_6$	1984 (t_{1u})		

[a] FTIR spectrum. [b] Outside CO laser range. [c] Obscured by parent band.

Experimental Section

Materials. $W(CO)_5$(4-CNpyr) was prepared photochemically via $W(CO)_5$(THF) (THF = tetrahydrofuran) following a published procedure[7] and purified by column chromatography on alumina. The 4-CNpyr ligand (Aldrich, 98%), methylcyclohexane (MCH, Aldrich, anhydrous

[†] University of Nottingham.
[‡] State University of New York.

(1) Wrighton, M. S.; Abrahamson, H. B.; Morse, D. L. *J. Am. Chem. Soc.* **1976**, *98*, 4105.
(2) Geoffroy, G. L.; Wrighton, M. S. *Organometallic Photochemistry*; Academic Press: New York, 1979.
(3) Lees, A. J. *Chem. Rev.* **1987**, *87*, 711.
(4) Moralejo, C.; Langford, C. H.; Sharma, D. K. *Inorg. Chem.* **1989**, *28*, 2205.
(5) Lees, A. J.; Adamson, A. W. *J. Am. Chem. Soc.* **1980**, *102*, 6874.
(6) Lees, A. J.; Adamson, A. W. *J. Am. Chem. Soc.* **1982**, *104*, 3804.
(7) Rawlins, K. A.; Lees, A. J.; Adamson, A. W. *Inorg. Chem.* **1990**, *29*, 3866.
(8) Wieland, S.; Van Eldick, R.; Crane, D. R.; Ford, P. C. *Inorg. Chem.* **1989**, *28*, 3663.
(9) With large spin–orbit coupling in W, the states are not pure singlets and triplets.
(10) Mabrouk, P. A.; Wrighton, M. S. *Inorg. Chem.* **1986**, *25*, 526.
(11) Perng, J.-H.; Zink, J. I. *Inorg. Chem.* **1990**, *29*, 1158.
(12) Morris, D. E.; Woodruff, W. H. In *Spectroscopy of Inorganic-based Materials*; Clark, R. J. H., Hester, R. E., Eds.; Wiley: New York, 1987.
(13) Glyn, P.; George, M. W.; Hodges, P. M.; Turner, J. J. *J. Chem. Soc., Chem. Commun.* **1989**, 1655.

0020-1669/91/1330-3543$02.50/0